

WAVELENGTHS OF SINGLE LAYER FOLDS: A COMPARISON BETWEEN THEORY AND OBSERVATION

JO-ANN SHERWIN and WILLIAM M. CHAPPLE

Department of Geological Sciences, Brown University,
Providence, Rhode Island 02912

ABSTRACT. The wavelength of 818 small, single layer folds from 6 locations was measured to test the Biot theory of fold wavelength-selection. The folds, mostly folded quartz veins in slate and phyllite, were chosen to fit as nearly as possible the assumptions of the Biot theory. The mean relative wavelengths of the fold groups (4.0 to 6.8) lead to ratios of layer viscosity to medium viscosity (2 to 8) which are too low for the Biot theory to be directly applicable.

A modified wavelength-selection theory takes into account the uniform shortening and thickening of the layer that accompanies the folding process. Using this theory, measured relative wavelengths, and estimated total amplification of the folding, it is possible to deduce the ratio of layer viscosity to medium viscosity and the total uniform shortening of the layer. Application to the folds studied gives viscosity ratios that range from 14 to 30 and uniform shortening and thickening that ranges from 1:2.7 to 1:5.7.

The large amounts of uniform shortening predicted are important both in considering the total amount of shortening represented by the folding and in considering some results of quartz fabric analyses of small folds.

INTRODUCTION

The Biot theory of the folding of stratified viscoelastic media (Biot, 1961) is important both for the insights it offers into the folding process and for the possibility it gives of determining viscosity ratios in folded rocks. The theory predicts that the wavelength of an isolated folded layer should be given by the relation:

$$L_d = 2\pi h \sqrt[3]{\frac{\eta}{6\eta_1}} \quad (1)$$

where L_d is the dominant wavelength, h is the thickness, η is the viscosity of the layer, and η_1 is the viscosity of the imbedding medium.

In the present study of naturally occurring folds, care was taken to choose folds that satisfied the assumptions of Biot: isolated, single-layer folds small enough so that gravity can be neglected. A large enough sample of folds was measured so that questions about the reproducibility of measurement and the distribution of natural fold wavelengths could be answered.

Biot, Odé, and Roever (1961) verified the predictions of the theory experimentally for materials of high viscosity ratio. Currie, Patnode, and Trump (1962) measured a number of fold wavelengths but did not restrict themselves to single-layer folds or to small folds. Kehle (1964) studied two folds in sea ice, where gravitational effects are important: one was consistent with Biot's theory if allowance was made for the measured shortening strain-rate in the ice, but the other was not in close agreement with the theory.

METHOD OF WAVELENGTH MEASUREMENT

Folded layers of hand specimen size, each of relatively uniform thickness and containing one to seventeen folds, were collected. Photographs were taken of a polished surface cut perpendicular to the fold axis. Larger fold trains were photographed at the outcrop. Measurements of layer thickness and arc length were taken from the photographs.

The total arc length of each fold train was measured by running a pair of dividers along the center line of the fold train. The average arc wavelength, L , was obtained by dividing the total arc length by the number of folds (one fold consists of one syncline plus one anticline, see fig. 1).

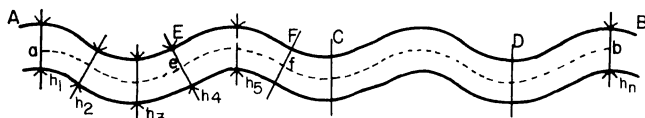


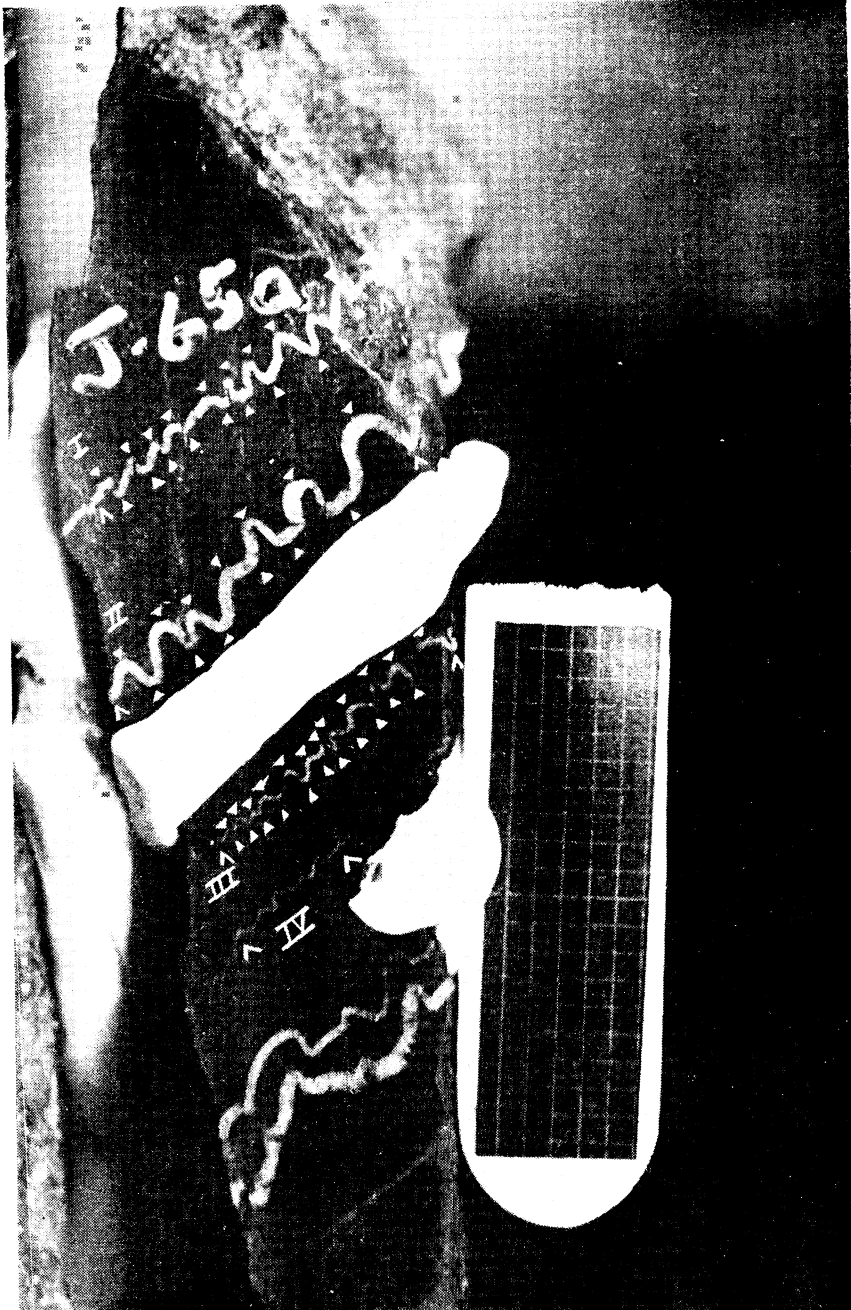
Fig. 1. Terminology used for measurements: AB = fold train; ab = total arc length along center line; CD = 1 fold; EF = one crest (or trough); ef = arc length of one crest (or trough) measured between midpoints of limbs of fold; h_1, h_2, \dots, h_n = thickness.

All discernible folds were counted regardless of amplitude; the lower limit of limb-dip required to form a recognizable fold was about 10° . Many of the fold trains were discontinuous due to small scale faulting (see pl. 1, fold trains I, III, IV). This, plus the small amplitude of many folds, caused difficulty in determining the number of folds present in each fold train (see pl. 1, fold train IV). Only fold trains for which the number of folds present was unambiguous were considered. Some fold trains showed thrusting parallel to the layer (see Cloos, 1964; and Ruedemann, 1942, p. 155, figs. 160, 161). The thrusting occurred after the fold wavelengths had asserted themselves and possibly contemporaneously with the folding. Such fold trains were measured in an "unthrust" configuration.

Thickness measurements perpendicular to the layer (usually five per fold) were averaged to give the average layer thickness, h (see fig. 1). The precise location of the edge of the layer was often difficult to determine, and the layers varied in thickness along their length (see pl. 1, fold train II). Most of the fold trains were quartz veins, and variation in thickness would be expected in an undeformed vein. With the possible exception of folds from the Delaware Water Gap, there was no consistent thickening in the crests and thinning in the limbs.

All the folds were actually elongate domes (the elongation direction being constant for a given outcrop), rather than being strictly two-dimensional. This was probably due to the initial shape perturbations being three-dimensional. The ratio of the wavelength parallel to the elongation to that perpendicular to the elongation is at least 5 so that a two dimensional theory is approximately correct.

PLATE 1



Folded quartz veins in phyllitic matrix from Sprague Upper Reservoir. Scale is in tenths of an inch. Total arc length was measured between arrows for fold trains I, II, III, IV. Dots indicate crests and troughs. The two layers at the bottom are not single layer folds and were not measured. See text for additional discussion.

Measurement of the arc wavelength (see fig. 1) of each crest and trough rather than the average arc wavelength of the folds in each fold train would be more closely related to the theory. To obtain such a measurement, the midpoints of fold limbs would have to be determined. This would lead to more frequent and more arbitrary choice of arc length end points than the method used. That L is a good approximation of the individual arc wavelength is substantiated by the fact that a histogram of L/h versus number of fold trains is the same as a histogram of L/h versus number of folds.

An average standard deviation, \bar{s} , of measurement of L/h was obtained to determine the reproducibility of the data. Seven fold trains exhibiting all degrees of imperfection of folding were measured seven times each, yielding $\bar{s} = 0.56$. Thus, it is approximately correct to say that a measured value of L/h is reproducible to within ± 1.12 for 95 percent of the hand specimen measurements. The error in outcrop measurements may be slightly greater due to lack of control of the outcrop surface and difficulty in aligning the film perpendicular to the fold axes.

RESULTS

The hand specimens from the Bellingham conglomerate (Carboniferous) were collected near Sprague Upper Reservoir, (Georgiaville Quadrangle, Rhode Island). These consisted of folded quartz veins in a light-gray sandy matrix and in a dark-gray phyllitic matrix (Richmond, 1952). Approximate composition of the two matrices was obtained by point counting. The sandy matrix consists of approximately 53 percent quartz, 46 percent muscovite, biotite, and chlorite, and 1 percent accessory minerals. The phyllitic matrix consists of approximately 43 percent quartz, 54 percent muscovite, biotite, and chlorite, and 3 percent accessory minerals. The thickness of the veins ranged from less than 0.01 inch to 0.5 inch. The veins are composed of subangular quartz grains with sutured contacts; the quartz does not show undulatory extinction. Minor amounts of biotite are found in the veins, most commonly close to the edges. Some veins are only one quartz grain thick. However, the continuity of the folds indicates that at the time of folding such a vein deformed as a continuum.

Figure 2 shows histograms of L/h versus number of folds for the two groups of Sprague Upper Reservoir folds. Both histograms are skew to the right. The mean L/h for both groups is given in table 1. For both groups, the mean L/h is much smaller and the range of L/h is much larger than that predicted by the Biot (1961) theory. Both groups were classed according to perfection of folding and according to thickness. No systematic variation of the mean and range of L/h was found.

Three groups of folds from the Taconic klippe in Vermont (Zen, 1961; Doll, 1961) were measured. Group 1 was collected from a road cut on Route 22A, 1 mile west of Poultney. The matrix is very dark gray slate. The fold trains are composed of quartz veins which range in thick-

SPRAGUE UPPER RESERVOIR FOLDS

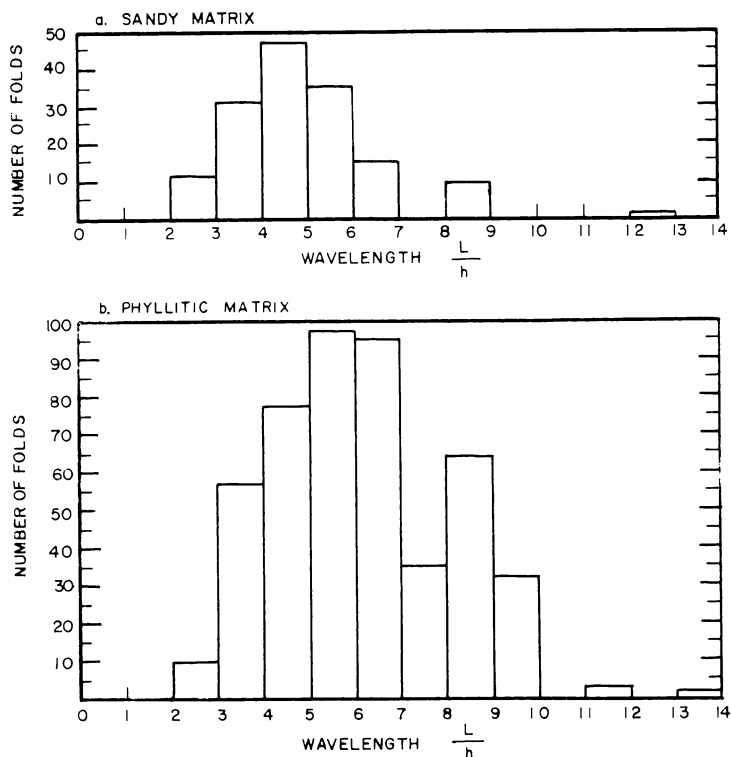


Fig. 2. Histograms of L/h versus number of folds for samples from Sprague Upper Reservoir: a. sandy matrix; b. phyllitic matrix.

ness from 0.01 inch to 0.3 inch. The quartz in the veins shows undulatory extinction, and magnetite crystals elongated parallel to the sides of the veins are found in the center of the veins.

Group 2 was collected from a road cut on Route 140, 1 mile east of East Poultney. The matrix is green slate. The folded layer is a quartzite bed with average thickness of 0.07 inch. The quartz grains in the layer are the same size as those in the matrix and show undulatory extinction. Calcite fragments are found in the layer and also scattered throughout the matrix.

Group 3 was collected from a road cut on Route 140 in East Poultney. The matrix is very dark gray slate. The fold trains are quartz veins which range in thickness from 0.01 inch to 0.2 inch.

Pictures were taken of fold trains in the Martinsburg Shale (Ordovician) exposed in a road cut on U.S. Route 46, 1.5 miles northeast of Belvidere, New Jersey, near the Delaware Water Gap. The layers ranged

in thickness from 2.5 inches to 6.5 inches. Maxwell (1962, p. 291) describes the Martinsburg at this locality as a slate containing folded layers of carbonate rich, dark gray siltstone.

Pictures were also taken of a fold train in the Nassau beds (lower Cambrian) exposed in a road cut on the road from Elizaville to Jackson Corners along the Roeliff Jansen Kill (Catskill, N. Y., Quadrangle). The layers ranged in thickness from 6 inches to 8.5 inches. Ruedeman (1942, p. 38) describes the Nassau beds at this locality as greenish or reddish and greenish shale slightly metamorphosed into phyllite containing folded greenish quartzite beds. Results of the measurement of all the groups of folds are tabulated in table I.

TABLE I

Sample	Number of folds	Mean wavelength L/h	$\frac{\eta}{\eta_1}$ (Biot theory) equation 1	Assumed amplification of L_d	$\frac{\eta}{\eta_1}$ (present theory)	Quadratic elongation Γ
Sprague Upper Reservoir						
phyllitic matrix	473	5.5	4	80	19	3.1
sandy matrix	142	4.5	2	80	14	4.1
Vermont						
group 1	82	5.2	3	80	17	3.3
group 2	9	6.8	8	200	30	2.7
group 3	83	5.1	3	80	17	3.4
Martinsburg Shale	12	4.0	2	200	15	5.7
Nassau Beds	17	5.7	4	200	23	3.3

FOLDING OF AN IMBEDDED SINGLE LAYER WHEN SHORTENING IS IMPORTANT

The relatively small dimensionless wavelengths, L/h , found in this study correspond to very low viscosity ratios (see table 1) when these ratios are calculated according to Biot's (1961) theory (equation 1). With these small viscosity ratios it is possible that a strong folding instability no longer exists, and it is certain that shortening of the layer during the folding may no longer be neglected. In the following, a modified theory which takes shortening into account is derived. In deriving the modified theory it will be sufficient to use thin plate theory (Biot, 1965, p. 426).

We consider the growth of a sinusoidal fold

$$W = A(t) \cos l x$$

of a single, linearly viscous layer imbedded in a medium of lesser viscosity. W is the vertical deflection of the layer, and X is horizontal distance along the layer. $A(t)$, the amplitude of the crest of the fold at time t , satisfies the equation (Biot, 1961, p. 1604)

$$\frac{\dot{A}}{A} = \frac{P}{\frac{4}{h} \frac{\eta_1}{l} + \frac{1}{3} \eta h^2 l^2} \quad (2)$$

where P is the longitudinal stress in the layer, and $l = 2\pi/L$ is the wavenumber. Since the layer shortens and thickens with time, h and l are functions of time. We neglect the difference in rate of thickening on the limbs and at the crests and assume that the shortening and thickening are those of a flat plate. With this assumption we find (Biot, 1965, p. 377):

$$h = h_0 e^{\frac{P}{4\eta} t}; \quad L = L_0 e^{-\frac{P}{4\eta} t}$$

The subscript zero specifies initial thickness or wavelength. (This assumption is valid only while the folds are of low amplitude, but it is shown below that most of the shortening takes place in the low-amplitude stages. In addition, most folds measured in this study do not show any noticeable thickening in the crests.)

Let us set:

$$n = \frac{\eta l}{\eta}, \quad \lambda = h l, \quad \lambda_0 = h_0 l_0, \quad \text{and} \quad \lambda = \lambda_0 \tau$$

where $\tau = e^{\frac{P}{2\eta} t}$ is the quadratic elongation associated with the shortening (Jaeger, 1962, p. 22; Brace, 1961). With this notation, equation 2 becomes:

$$\frac{\dot{A}}{A} = \frac{P}{\eta} \frac{1}{\frac{\lambda_0^2 \tau^2}{3} + \frac{4n}{\lambda_0 \tau}} \quad (3)$$

Biot (1965, p. 427) solves this equation approximately for small total shortening; the solution derived below is not so restricted. If time is measured by the quadratic elongation of the shortening and variables are separated, equation 3 can be written as:

$$\frac{dA}{A} = \frac{\lambda_0 d\tau}{2n + \frac{1}{6} \lambda_0^3 \tau^3}$$

The integral of this equation is:

$$\ln \frac{A}{A_0} = \int_1^T \frac{\lambda_0 d\tau}{2n + \frac{1}{6} \lambda_0^3 \tau^3} \quad (4)$$

where A_0 is the amplitude when the quadratic elongation is one and T is the final value of the quadratic elongation.

To find the dominant wavenumber, that is, that wavenumber whose cumulative amplification is largest, we differentiate the right hand side of equation 4 with respect to λ_0 and set the derivative equal to zero. This gives:

$$\lambda_0^3 = 12n \frac{1}{T(T+1)} \quad (5)$$

or in a form more convenient for comparison with the observed final wavelength and thickness:

$$\lambda^3 = \lambda_0^3 \tau^3 = 12 n \frac{T^2}{T+1} \quad (6)$$

When the shortening of the layer can be measured directly, equation 6 may be used to determine the viscosity ratio; when it cannot, it is more convenient to estimate the amplification at the dominant wavelength than the shortening.

Substituting the value of λ_0 given by equation 5 into equation 4, we obtain for the amplification of the dominant wavelength:

$$\ln \frac{A}{A_0} = \frac{1}{n^{2/3}} \left[\frac{3}{2T(T+1)} \right]^{1/3} \int_1^T \frac{d\tau}{1 + \frac{\tau^3}{T(T+1)}} \quad (7)$$

This integral can be evaluated by elementary means; figure 3 was obtained by evaluating equations 6 and 7 for a series of values of n and T .

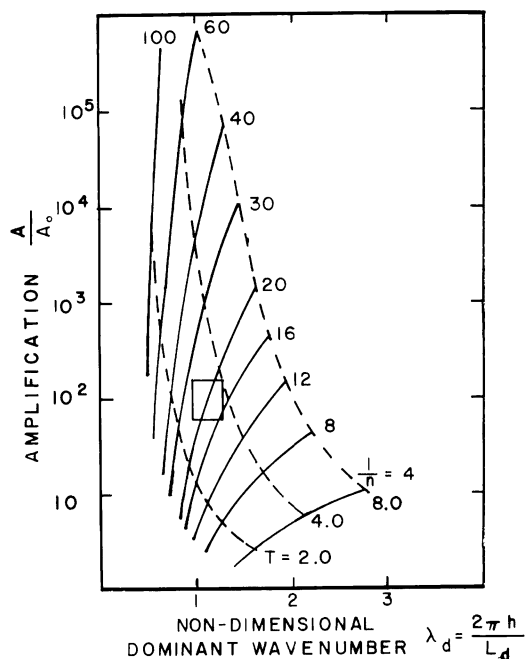


Fig. 3. Amplification of the dominant wavelength as a function of the non-dimensional dominant wavenumber for various values of viscosity ratio $1/n = \eta/\eta_1$ and quadratic elongation of the uniform shortening T . As a layer-medium system of given viscosity ratio is compressed its non-dimensional dominant wavenumber and the amplification of this dominant wavenumber increase as shown by the solid curves. The dashed curves represent the quadratic elongation of the layer corresponding to a given dominant wavenumber and its total amplification. The small rectangle indicates the estimates of the non-dimensional dominant wavenumber and its amplification for the Sprague Upper Reservoir phyllitic matrix folds.

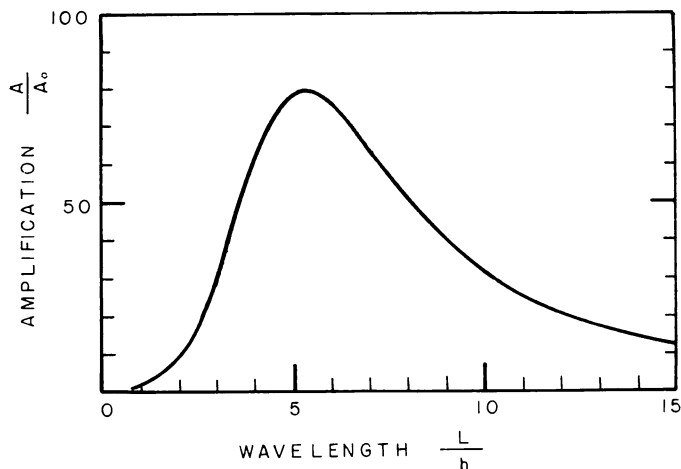


Fig. 4. Amplification as a function of wavelength for a viscosity ratio of 18 and a quadratic elongation of the layer of 3.2. (These values are approximately those of the Sprague Upper Reservoir phyllitic matrix folds.) The peak of the curve represents the dominant wavelength for this viscosity ratio and quadratic elongation.

For a given population of natural folds, the dominant wavelength can be measured and the amplification of the dominant wavelength can be estimated on geological grounds; an estimate of the viscosity ratio can then be obtained from figure 3. For example, for the Sprague Upper Reservoir phyllitic matrix folds of the present study, the amplification is estimated below to lie between 60 and 150, and the dominant wavenumber is estimated to lie between 0.97 and 1.26. The small rectangle in figure 3 then provides estimates of the viscosity ratio of the folds and the amount of uniform shortening which has occurred. When the viscosity ratio is greater than 100, figure 3 shows that the dominant wavenumber is almost independent of the amplification; this is the range in which the theory of Biot (1961) is applicable.

Equation 4 can be used to calculate the variation of amplification with wavenumber—or equivalently with wavelength—when shortening and viscosity ratio are held fixed. Figure 4 shows this variation when the shortening and viscosity ratio are those estimated for the Sprague Upper Reservoir phyllitic matrix folds.

Band widths derived from the present theory are larger than those derived from the Biot theory (Biot, 1961, p. 1606). This is to be expected since when shortening is taken into account there is a range of wavelengths that had the highest growth rate at a particular stage of the folding process.

APPLICATION OF THE THEORY TO THE OBSERVED FOLDS

When the original unfolded layer is a quartz vein, it seems reasonable that it had initial shape perturbations with limb-dips up to 1 or 2

degrees. Perturbations of this size would have an amplitude of 0.05 h to 0.1 h if they had an initial wavelength of 17 h, that of the Sprague Upper Reservoir phyllitic-matrix folds. As discussed above, some of the measured folds have limb-dips as small as 10 to 20°; therefore, it is possible that some of the measured folds have been amplified by a factor of only 10 or 20. Corresponding to this estimate of minimum amplification, it seems likely that the amplification of the dominant wavelength ranges from 60 to 150. As outer limits, we might place the amplification between 40 and 400. Thus (see fig. 3) the viscosity ratio for these folds probably lies between 16 and 21 and almost certainly lies between 14 and 30.

When the original layer is a sedimentary bed rather than a quartz vein, it may have a flatter initial shape and show correspondingly greater amplification.

An additional check on these estimates can be obtained by considering the spread of observed wavelengths from the Sprague Upper Reservoir phyllitic matrix folds. Comparing the amplification expected at a given wavelength (fig. 4) with the number of folds with certain ranges of wavelength (fig. 2), we find that 9 of the 473 folds have wavelengths corresponding to an amplification of 15 to 20; 188 have wavelengths corresponding to an amplification of 20 to 60; and the remaining 276 have wavelengths corresponding to an amplification of 60 to 80.

The shape of the amplification curve (fig. 4) should be similar to the shape of the distribution curve of observed folds versus wavelength (fig. 2). A given shape perturbation will be observed as a fold only if its initial amplitude times its amplification produces a limb-dip of 10 or 15°; if the amplitudes of the initial perturbations are independent of wavelength, the observed number of folds with a given wavelength is proportional to the amount that wavelength is amplified. The exact relation between the shapes of the two curves will depend on the statistical characteristics of the initial shape perturbations, but general features of the curves, such as their asymmetry, should be similar. Comparison of figure 4 and figure 2 shows that this is true. (If wavenumber, rather than wavelength is chosen as the independent variable for the two curves, the asymmetry is still similar.)

Wavelengths and viscosity ratios for the various groups of folds are tabulated in table 1. For locations other than Sprague Upper Reservoir, the estimated dominant wavelengths are rather crude since not enough folds were available for measurement. The fact that the viscosity ratios and shortening derived for these other folds is similar to those from the Sprague Upper Reservoir folds does suggest that these might be typical values for single layer folds. The lower viscosity ratio of the sandy matrix folds from Sprague Upper Reservoir indicates that the sandy matrix is more competent than the phyllitic matrix; this agrees with the observed structural styles of the two rock-types.

DISCUSSION

All of the groups of folds measured in the present study show relatively low ratios of dominant wavelength to thickness, L_d/h ; in fact, these ratios are too low for the Biot theory to be applicable (Biot, 1961, p. 1606-7). When the measured wavelengths are compared with the modified theory presented here, relatively low viscosity ratios, η/η_1 , and relatively large amounts of shortening are found. The total amplification at the dominant wavelength was deduced on geological grounds to be appreciably smaller than that postulated by Biot; the correctness of this deduction is supported by the agreement between the predicted and observed spread in wavelength for the Sprague Upper Reservoir phyllitic matrix folds.

The large amount of uniform shortening implied by the observed fold wavelengths is probably a consequence of the hypothesis of linear viscosity (compare Biot, 1961, p. 1611). The existence of the shortening could be checked directly by the use of geologic strain-indicators such as deformed oölites; such a study would have important implications in determining the rheology of natural folds.

If the hypothesis of linear viscosity—and the shortening that it implies—are correct, there are significant geologic consequences. For example:

1. Maxwell (1962) estimates from the shape of folded layers that a shortening of 40 percent accompanied the production of slaty cleavage in the Delaware Water Gap. (A “shortening” of 40 percent is equivalent to a quadratic elongation of 2.8; that is, an original sphere is deformed into an ellipsoid with a ratio of major axis of 2.8:1). If we add in the uniform shortening accompanying the folding (table 1), the total shortening is 75 percent (quadratic elongation of 16). The larger figure for the shortening would seem to be in better accord with the well-developed similar folds (Maxwell, 1962, p. 286) in the Martinsburg Shale of the Delaware Water Gap region.

2. The major portion of the shortening occurs during the low-dip stages of folding where it is relatively uniform along the length of the fold. For example, a layer with a viscosity ratio of 18 and initial limb-dips of 0.87° will have 20° limb-dips when the quadratic elongation within the layer is 2.6. While the layer undergoes a further quadratic elongation of 1.4 its limb-dips increase to 50° . (In fact, since this additional shortening will not be uniform along the length of the layer, it is dealt with only approximately by the present theory.)

Studies of the finite strains in well-defined natural folds are not available for comparison with this predicted shortening, but studies of the strains recorded in calcite twin lamellae and dynamic analyses of quartz deformation lamellae in folds are available (Carter and Friedman, 1965; Hansen and Borg, 1962; Scott, Hansen, and, Twiss 1965). (The folds analyzed in the first two of these studies are so large that gravity may have

been important in their formation, so that their results apply only approximately to the present study.)

In each of these studies the maximum compressive stress axis is sub-parallel to the plane of bedding and sub-perpendicular to the fold axis. The authors of these studies suggest two possible interpretations for the development of the twins and deformation lamellae.

1. Lamellae and twins are formed before folding or in the early stages of folding and then passively rotated in the limbs of the folds to their present position.

2. Lamellae and twins are formed late in the folding process, but the maximum compressive stress is still approximately parallel to bedding in the competent layers studied.

The large amount of uniform shortening in the early stages of folding predicted by the present study seems to support interpretation 1. However, since the present analysis is only valid for low dips, it cannot be used to assess the validity of interpretation 2. In addition, the preservation of a fabric formed during the early stages of folding through the later stages is difficult to understand. One possibility is that the stresses are relatively lower when the limb-dips are higher: In Chapple (1966) it is shown that when an isolated layer is being folded the compressive stress in the layer must decrease as the fold amplitude grows if the rate of approach of adjacent crests and troughs is not to become unreasonably large.

ACKNOWLEDGMENTS

The authors wish to thank Dr. Jeanne Gilbert for the use of her camera and Professor Bruno J. Giletti for critical reading of the manuscript. This research was supported by the Advanced Research Projects Agency under contract SD-86.

REFERENCES

- Biot, M. A., 1961, Theory of folding of stratified viscoelastic media and its implications in tectonics and orogenesis: *Geol. Soc. America Bull.*, v. 72, p. 1595-1620.
- 1965, Mechanics of incremental deformations: New York, John Wiley and Sons, Inc., 504 p.
- Biot, M. A., Ode, Helmer, and Roever, W. L., 1961, Experimental verification of the theory of folding of stratified viscoelastic media: *Geol. Soc. America Bull.*, v. 72, p. 1621-1632.
- Brace, W. F., 1961, Mohr construction in the analysis of large geologic strain: *Geol. Soc. America Bull.*, v. 72, p. 1059-1080.
- Carter, N. L., and Friedman, M., 1965, Dynamic analysis of deformed quartz and calcite from the Dry Creek Ridge anticline, Montana: *Am. Jour. Sci.*, v. 263, p. 747-785.
- Chapple, W. M., 1966, Fold shape and rheology: folding of a viscous plastic layer: [abs.]: *Am. Geophys. Union Trans.*, v. 47, p. 189-190.
- Cloos, E., 1964, Wedging, bedding plane slips, and gravity tectonics in the Appalachians, in *Tectonics of the southern Appalachians*: Virginia Polytech. Inst. Dept. of Geol. Studies Mem. 1, p. 216-261.
- Currie, J. B., Patnode, H. W., and Trump, R. P., 1962, Development of folds in sedimentary strata: *Geol. Soc. America Bull.*, v. 73, p. 655-674.
- Doll, C. G., Cady, W. M., Thompson, J. B., Jr., and Billings, M. P., 1961, Centennial geologic map of Vermont: Vermont Geol. Survey.
- Hansen, E. C., and Borg, I. Y., 1962, The dynamic significance of deformation lamellae in quartz of a calcite-cemented sandstone: *Am. Jour. Sci.*, v. 260, p. 321-336.

- Jaeger, J. C., 1962, *Elasticity, fracture, and flow*, 2nd ed.: New York, John Wiley and Sons, Inc., 208 p.
- Kehle, R. O., 1964, Deformation of the Ross Ice Shelf, Antarctica: *Geol. Soc. America Bull.*, v. 75, p. 259-286.
- Maxwell, J. C., 1962, Origin of slaty and fracture cleavage in the Delaware Water Gap Area, New Jersey and Pennsylvania, *in* *Petrologic studies—a volume in honor of A. F. Buddington*: New York, Geol. Soc. America, p. 281-311.
- Richmond, G. M., 1952, Bedrock geology of the Georgiaville quadrangle, Rhode Island: U.S. Geol. Survey Geol. Quadrangle Map GQ-16.
- Ruedemann, Rudolph, 1942, Geology of the Catskill and Kaaterskill quadrangles, pt. I: New York State Mus. Bull. 331, p. 584-594.
- Scott, W. H., Hansen, E. C., and Twiss, R. J., 1965, Stress analysis of quartz deformation lamellae in a minor fold: *Am. Jour. Sci.*, v. 263, p. 729-746.
- Zen, E-an, 1961, Stratigraphy and structure at the north end of the Taconic Range in west-central Vermont: *Geol. Soc. America Bull.*, v. 72, p. 293-338.